Periodic gravitational lensing by oscillating boson stars

Xing-Yu Yang,^{1,*} Tan Chen,^{2,3,†} and Rong-Gen Cai^{4,‡}

¹Quantum Universe Center (QUC), Korea Institute for Advanced Study, Seoul 02455, Republic of Korea

²Institute for Frontier in Astronomy and Astrophysics,

Beijing Normal University, Beijing 102206, China

³School of Physics and Astronomy, Beijing Normal University, Beijing 100875, China ⁴Institute of Fundamental Physics and Quantum Technology, Ningbo University, Ningbo 315211, China

We show that oscillating (real-scalar) boson stars can act as strictly periodic gravitational lenses and generically host an *oscillating radial caustic*. Sources near this caustic cross it every half period, producing achromatic phase-locked photometric spikes synchronized with an astrometric wobble, providing a promising target for time-domain astronomy. Event-number estimation indicates a measurable discovery space with current astrometric and high-cadence photometric surveys. These predictions rely only on the dynamics of long-lived real-scalar condensates, therefore offering a clean test of self-gravitating quantum fields in curved spacetime. The framework extends naturally to self-interacting real scalars (including axion-like particles) and to ultralight vector bosons.

Introduction. Boson stars are self-gravitating condensates of quantum fields whose pressure support is provided not by thermal motion, as in ordinary stars, but by the Heisenberg uncertainty principle and (when present) self-interactions of the field. Originally proposed for complex scalar fields in the 1960s [1], they have since been explored across a wide range of particle-physics models, from ultralight axions to Higgs-portal scalars, and at masses spanning many orders of magnitude. Because their spacetime is entirely determined by well-understood quantum and gravitational physics, boson stars serve as clean theoretical laboratories for testing strong-gravity effects and dark-matter phenomenology. They also provide a compelling alternative to black holes in certain astrophysical contexts and a natural end-state for darkmatter collapse, making them an object of enduring interest in both high-energy theory and observational astronomy [2-5].

A particularly intriguing subset is the class of oscillating boson stars, built from a real scalar field [6]. In the absence of a global U(1) symmetry, the field cannot maintain a static phase; instead, the entire configuration oscillates coherently at a fundamental frequency slightly below the particle mass, giving rise to long-lived, nonsingular, asymptotically-flat solutions known as oscillatons [7–9]. This intrinsic time dependence modulates the star's density profile and gravitational potential, imprinting periodic signatures on any passing radiation or orbiting body. Such oscillating boson stars therefore offer a unique observational handle: unlike their complex-scalar counterparts, they can in principle be identified through periodic photometric and astrometric signals, providing a new avenue for probing the particle nature of dark matter and the dynamics of self-gravitating quantum fields

* Corresponding author: xingyuyang@kias.re.kr

in curved spacetime.

Gravitational lensing provides a sensitive probe for compact masses. If the lens potential itself varies periodically, as expected for an oscillating boson star, the magnification and apparent position of a background source inherit the same periodicity. Moreover, an oscillating boson star is an extended nonsingular lens and therefore possesses radial caustic whose size pulsates with the stellar oscillation. Whenever a source crosses this caustic, its magnification jumps dramatically by orders of magnitude, and a close pair of bright images either annihilates at or emerges from the critical curve [10–12]. A source that repeatedly encounters an oscillating caustic will thus display a train of synchronous astrometric and photometric spikes. Detecting such a periodic sequence would constitute compelling evidence for an underlying oscillating boson star, while a null search would constrain their abundance over wide mass ranges. We set $c = \hbar = G = 1$ throughout the paper.

Gravitational lensing. For a spherically symmetric configuration, the metric can be written as

$$ds^{2} = -B(t, r)dt^{2} + A(t, r)dr^{2} + r^{2}(d\vartheta^{2} + \sin^{2}\vartheta d\varphi^{2}), (1)$$

with two time-dependent metric functions A(t,r) and B(t,r). A minimally coupled massive real scalar field ϕ evolving in a curved background is governed by the Einstein-Klein-Gordon (EKG) equations $G_{ab} = \kappa T_{ab}$ and $\nabla^a \nabla_a \phi = m^2 \phi$, which have solutions of the form [6]

$$A(t,r) = 1 + \sum_{j=0}^{j_{\text{max}}} A_{2j}(r) \cos(2j\omega t),$$
 (2a)

$$B(t,r) = 1 + \sum_{j=0}^{j_{\text{max}}} B_{2j}(r) \cos(2j\omega t),$$
 (2b)

$$\phi(t,r) = \sum_{j=1}^{j_{\text{max}}} \phi_{2j-1}(r) \cos([2j-1]\omega t), \qquad (2c)$$

[†] Corresponding author: chentan@bnu.edu.cn

[‡] Corresponding author: caironggen@nbu.edu.cn

where ω is the fundamental frequency and j_{max} is the mode at which the Fourier series is truncated. Substituting these series into the EKG equations and matching terms of the same frequency yield a set of coupled ordinary differential equations for the radial coefficients. The boundary conditions are determined by requiring asymptotic flatness and central regularity, which are: (i) asymptotic flatness requires $\phi|_{r\to\infty}\to 0$ and $\{A,B\}|_{r\to\infty}\to 1$; (ii) central regularity implies $\partial_r \phi|_{r=0} = 0$ and $A|_{r=0} = 1$. Introducing the dimensionless variables $\tilde{t} \equiv mt$, $\tilde{r} \equiv mr$, $\phi \equiv \sqrt{\kappa} \phi$ and $\tilde{\omega} \equiv \omega/m$, one finds that for every value of $\phi_1(0)$ a solution exists [6–9]. The mass of oscillating boson stars is given by $M = \tilde{M}/m$ with dimensionless mass $\tilde{M} \equiv \lim_{\tilde{r}\to\infty} \tilde{r}[1-A(\tilde{t},\tilde{r})^{-1}]/2$, which has a maximum value $\tilde{M}_{\rm max} \approx 0.6$ by requiring stability of stars. Because the Fourier expansion converges rapidly, we retain only the leading oscillatory terms and set $j_{\text{max}} = 1$.

Photon trajectories follow null geodesics. Restricting to the equatorial plane $(\theta = \pi/2)$, a geodesic is specified by the time \hat{t} and radius \hat{r} of closest approach, which together determine the deflection angle $\hat{\alpha}$. In FIG. 1, we show the corresponding deflection angle as a function of $\{\hat{t},\hat{r}\}\$ for a representative oscillating boson star with M=0.5, which gives $\tilde{\omega} \approx 0.95$. Because the metric oscillates with frequency 2ω , the deflection angle oscillates with period $T = \pi/\omega$, which will produce astrometric and photometric variations of the lensed images. For a given \hat{t} , there is a characteristic radius r_c . For $\hat{r} \gg r_c$ the metric approaches the Schwarzschild form which leads to $\hat{\alpha} \approx 4M/\hat{r}$, whereas for $\hat{r} \ll r_{\rm c}$ the central regularity gives $\hat{\alpha} \propto \hat{r}$. We find that the numerical results of the deflection angle are well described by a broken power-law form

$$\hat{\alpha}(\hat{t},\hat{r}) = \frac{2r_{\rm Sch}\,\hat{r}}{r_{\rm c}(\hat{t})^2} \left[1 + \left(\frac{\hat{r}}{r_{\rm c}(\hat{t})}\right)^{1/\Delta} \right]^{-2\Delta},\tag{3}$$

where $r_{\rm Sch} \equiv 2M$, and $\Delta \approx 1/4$ with slight changes depending on the specific star configuration. Due to intrinsic stellar oscillations, the characteristic radius $r_{\rm c}$ also periodically varies. In the following, we adopt this parametrization of the deflection angle, which captures the essential physics while remaining analytically tractable.

The lensing geometry is described by the lens equation

$$\beta = \theta - \alpha,\tag{4}$$

where β is the (unobservable) angular separation of the source from the optical axis (chosen for convenience along the lens direction), $\theta \equiv \hat{r}/D_{\rm OL}$ is the observed angular position of an image, and $\alpha \equiv \hat{\alpha}(1-D_{\rm OL}/D_{\rm OS})$ is the reduced deflection angle. Here $D_{\rm OL}$ and $D_{\rm OS}$ are the observer-lens and observer-source distances, respectively. Introducing the length scale $R \equiv \sqrt{2r_{\rm Sch}D}$ with $D \equiv D_{\rm OL}(D_{\rm OS}-D_{\rm OL})/D_{\rm OS}$, the lens equation can be cast in

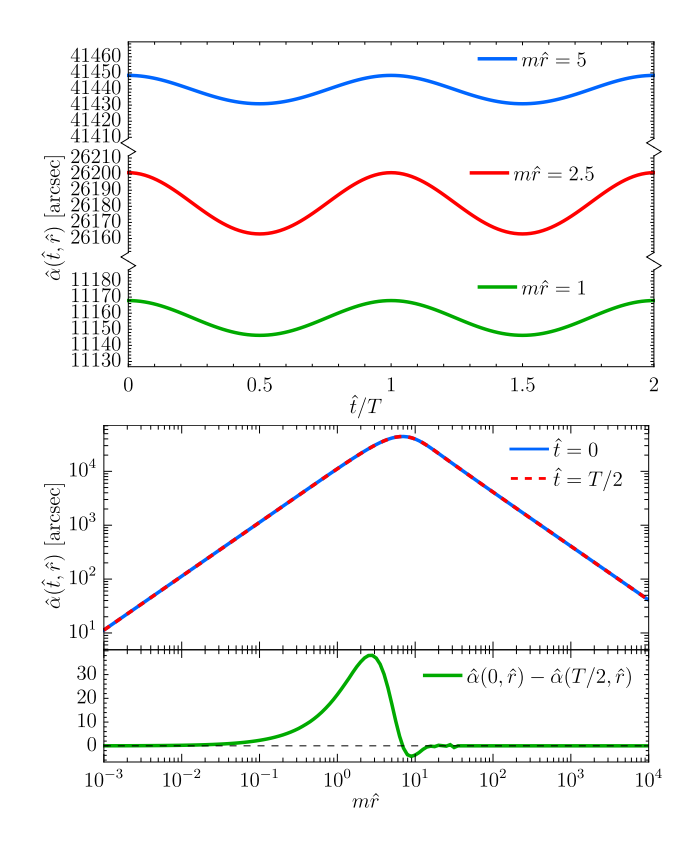


FIG. 1. Deflection angle $\hat{\alpha}$ as a function of $\{\hat{t}, \hat{r}\}$ for the oscillating boson star with $\tilde{M} = 0.5$.

dimensionless form

$$y = x - \nu^{-2}x \left[1 + (x/\nu)^4\right]^{-1/2},$$
 (5)

with $y \equiv \beta D_{\rm OL}/R$, $x \equiv \theta D_{\rm OL}/R$, and $\nu \equiv r_{\rm c}/R$. Because the characteristic radius $r_{\rm c}$ oscillates, $\nu(t)$ is periodic in time. We model its time dependence as $\nu(t) = \bar{\nu}[1 - \varepsilon \cos(2\pi t/T)]$, where ε depends only on \tilde{M} and $\bar{\nu}$ depends on \tilde{M} and $\tilde{D} \equiv mD$.

Periodic caustic-crossing lensing. From the dimensionless lens equation (5) it follows that, for $\nu > 1$, no caustic forms and every source position produces a single image. When $\nu < 1$, a radial caustic appears: a source outside the caustic yields one image, a source on the caustic produces two images, and a source inside the caustic gives three images. Because $r_{\rm c}$ oscillates and $y_{\rm cau}(\nu)$ is monotonically decreasing, the caustic periodically pulsates in and out. A source located near this caustic consequently crosses it once every half period. Each crossing induces a sharp magnification spike and the sudden creation or annihilation of a bright image pair. Figure 2 presents a schematic illustration of this periodic caustic-crossing lensing produced by an oscillating boson star. A background source that repeatedly traverses an oscillating caustic therefore exhibits a sequence of synchronous astrometric and photometric spikes; detecting such a pattern would constitute strong evidence for an underlying oscillating boson star.

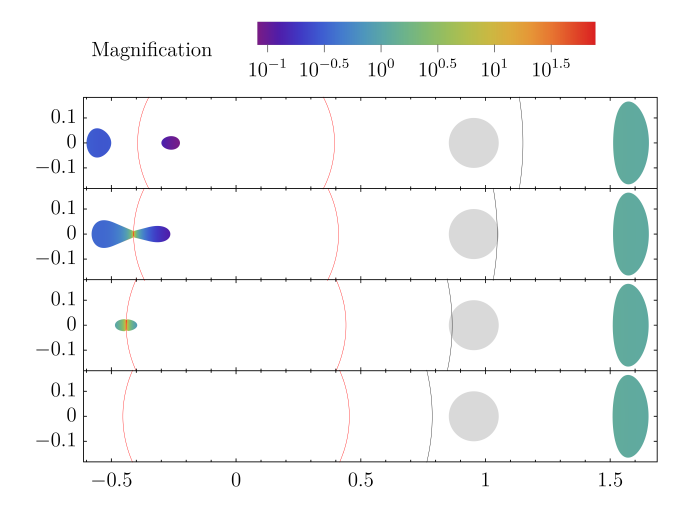


FIG. 2. Schematic of periodic caustic-crossing lensing by an oscillating boson star. The gray disk marks the (unresolved) source; the black and red curves indicate the radial caustic and its corresponding radial critical curve, respectively. From top to bottom, the panels show successive phases over half an oscillation period as the caustic contracts. Phase 1 (top): the source lies entirely inside the caustic and three distinct images are produced. Phase 2: as the caustic moves inward, part of the source lies outside it and the image pair near the critical curve approaches and brightens. Phase 3: continued contraction further shrinks the image pair. Phase 4 (bottom): the source is entirely outside the caustic; the pair annihilates at the critical curve, leaving a single image.

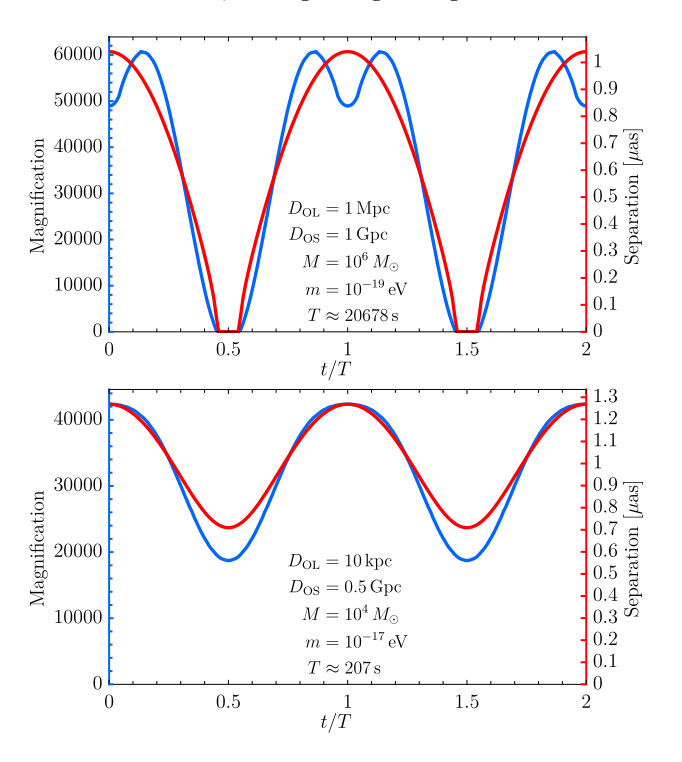


FIG. 3. Time evolution of the image pair for two representative lensing configurations. The blue curve shows the mean magnification of the image pair (left blue axis), and the red curve shows the pair's maximum radial separation (right red axis).

In FIG. 3 we show the time evolution of the image pair for two representative lensing configurations. Top panel: an oscillating boson star with $M=10^6\,M_\odot$ and $m = 10^{-19} \,\mathrm{eV}$ (period $T \approx 20678 \,\mathrm{s}$) at $D_{\mathrm{OL}} = 1 \,\mathrm{Mpc}$ lenses a solar-radius source with uniform surface brightness at $D_{OS} = 1$ Gpc, i.e., both lens and source lie outside the Milky Way. Here the angular extent of the source is smaller than the angular excursion of the caustic, so the system passes through all four phases. The blue curve shows the mean magnification of the image pair; the red curve shows its maximum radial separation. The magnification cycles from $\mathcal{O}(10^4)$ down to 0, while the radial separation oscillates from μ as scales to 0. Such extreme magnifications make detection feasible even on cosmological scales, as demonstrated by the $\mathcal{O}(10^3)$ magnification of an individual star at redshift 1.5 by a galaxycluster lens [13]. Bottom panel: lens $(M = 10^4 M_{\odot})$ $m = 10^{-17} \,\mathrm{eV}, T \approx 207 \,\mathrm{s}$) at $D_{\mathrm{OL}} = 10 \,\mathrm{kpc}$, with source at $D_{\rm OS} = 0.5\,{\rm Gpc}$ (lens inside, source outside the Milky Way). Here the source's angular size exceeds the caustic's excursion, and the source position is chosen so that the system samples phases 2 and 3 only. Because phase 4 does not occur, the minimum magnification and separation remain nonzero.

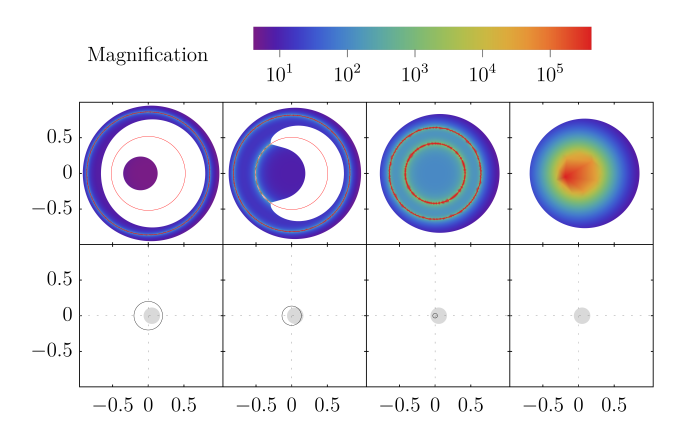


FIG. 4. Schematic of type II periodic caustic-crossing lensing by an oscillating boson star. The gray disk marks the (unresolved) source; the black curve shows the radial caustic and the inner red curve is the corresponding radial critical curve; the outer red curve denotes the Einstein ring. Panels (left to right) show successive phases over half an oscillation period as the caustic contracts. Phase 1 (left): the source lies entirely inside the caustic; a bright Einstein ring and a central image are present. Phase 2: as the caustic moves inward, part of the source lies outside it and the image pair near the critical curve approaches and brightens. Phase 3: the radial caustic is fully contained within the source; the Einstein ring merges with the central image, producing two bright rings: the outer Einstein ring and the inner radial-critical ring. Phase 4 (right): the caustic vanishes ($\nu > 1$); the bright rings disappear, leaving a single image with a bright central region.

For an extended source, a second type of periodic lensing arises when the source covers the lens center, as il-

lustrated in FIG. 4. We refer to this as type II periodic caustic-crossing lensing, in contrast to type I in FIG. 2 where the source does not cover the lens center. In the type II case, whenever a caustic is present, an Einstein ring forms, and the resulting image morphology differs markedly from type I.

Event number. For periodic caustic-crossing lensing to occur, two conditions must be satisfied: (i) an oscillating radial caustic must exist, i.e. $\nu_{\min} < 1$, which implies

$$D_{\rm OL} > r_{\rm cS},$$
 (6a)

$$D_{\rm OS} > D_{\rm OL}^2 / (D_{\rm OL} - r_{\rm cS}),$$
 (6b)

where $r_{\rm cS} \equiv r_{\rm c,min}^2/(2r_{\rm Sch})$; (ii) the source must intersect the caustic at some phase, which constrains its angular position to $\beta_{\rm min} < \beta_{\rm src} < \beta_{\rm max}$, with

Type I:
$$\begin{cases} \beta_{\min} = \max[\frac{R_{\text{src}}}{D_{\text{OS}}}, \, \beta_{\text{cau}}(\nu_{\max}) - \frac{R_{\text{src}}}{D_{\text{OS}}}], \\ \beta_{\max} = \beta_{\text{cau}}(\nu_{\min}) + \frac{R_{\text{src}}}{D_{\text{OS}}}, \end{cases}$$
(7a)

$$\text{Type II}: \begin{cases} \beta_{\min} = \max[0, \ \beta_{\text{cau}}(\nu_{\max}) - \frac{R_{\text{src}}}{D_{\text{OS}}}], \\ \beta_{\max} = \frac{R_{\text{src}}}{D_{\text{OS}}}, \end{cases}$$
(7b)

where $R_{\rm src}$ is the source radius and $\beta_{\rm cau}(\nu) = y_{\rm cau}(\nu)R/D_{\rm OL}$ denotes the angular radius of the radial caustic.

Assuming the survey volume extends out to a distance Z, and denoting by n_a and n_b the number densities of oscillating boson stars and sources, respectively, the expected number of periodic caustic-crossing lensing events is

$$N_{\text{evt}} = \int_{0}^{Z} dD_{\text{OL}} \left\{ n_{a} \Theta(D_{\text{OL}} - r_{\text{cS}}) 4\pi D_{\text{OL}}^{2} \right.$$

$$\times \int_{D_{\text{OL}}}^{Z} dD_{\text{OS}} \left\{ n_{b} \Theta(D_{\text{OS}} - \frac{D_{\text{OL}}^{2}}{D_{\text{OL}} - r_{\text{cS}}}) \right.$$

$$\times 2\pi D_{\text{OS}}^{2} \max \left[0, \cos \beta_{\min} - \cos \beta_{\max} \right] \right\}$$

$$\equiv \left(\frac{n_{a}}{\text{kpc}^{-3}} \right) \left(\frac{n_{b}}{\text{kpc}^{-3}} \right) \mathcal{N}(m, M, Z, R_{\text{src}}),$$
(8)

where $\Theta(x)$ is the Heaviside step function. For type I the inequality $\beta_{\min} < \beta_{\max}$ is automatically satisfied. For type II it imposes $\beta_{\text{cau}}(\nu_{\max}) < 2R_{\text{src}}/D_{\text{OS}}$, which sets an additional upper bound on D_{OS} . Since in practical surveys $R_{\text{src}} \ll Z$, the effective upper limit of the D_{OS} integral is much smaller than Z, implying that the type II event yield is far below the type I yield. Accordingly, we focus on type I in the remainder of this section.

Figure 5 displays the reduced event number \mathcal{N} for a range of parameter choices. The upper boundary corresponds to the stability limit $M_{\rm max} = \tilde{M}_{\rm max}/m \approx$

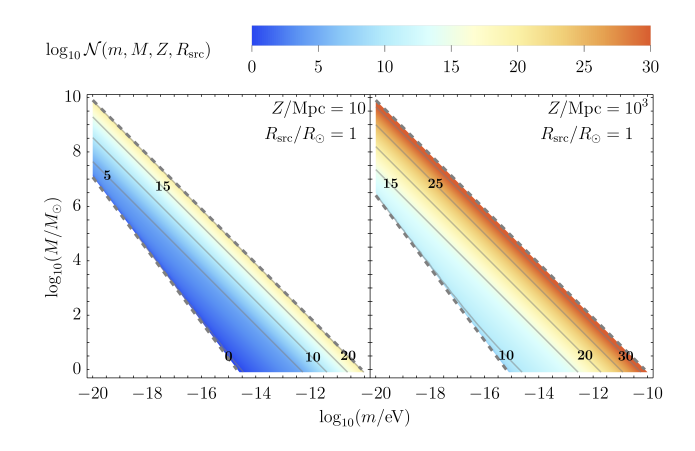


FIG. 5. Reduced event number \mathcal{N} for type I periodic caustic-crossing lensing as a function of model parameters.

 $8 \times 10^9 \, M_{\odot} \, (10^{-20} \, \text{eV/m})$, while the requirement of a radial caustic (ν < 1) gives the lower bound $M_{\rm min} \approx 1.6 \times 10^7 \, M_{\odot} \, (Z/4 \, / \, {\rm Mpc})^{-1/3} \, (10^{-20} \, {\rm eV}/m)^{4/3}$. These bounds are indicated by the dashed lines. The parametric dependence of the reduced event number can be written approximately as $\mathcal{N}(m, M, Z, R_{\rm src}) \sim$ $Z^6F_1(M)F_2(R_{\rm src})$, where $F_2(R_{\rm src}) \sim \mathcal{O}(1)$ for realistic stellar sizes. This scaling is intuitive: the volume integral $\int^Z D_{\rm OL}^2 {\rm d}D_{\rm OL} \int^Z D_{\rm OS}^2 {\rm d}D_{\rm OS}$ contributes the Z^6 factor; the lensing configuration, which is scale-invariant under m, supplies the $F_1(M)$ dependence; and the practical regime $R_{\rm src} \ll D$ makes $F_2(R_{\rm src})$ order unity. For a survey extending to $Z = 1 \,\mathrm{Gpc}$, the reduced event number \mathcal{N} can be as large as $\mathcal{O}(10^{30})$, which implies a correspondingly large event number N_{evt} once realistic values of n_a and n_b are applied. This estimate counts all periodic caustic-crossing events irrespective of image brightness: consequently, a substantial fraction will be too faint for current facilities.

To estimate the number of detectable events for current facilities, consider a solar-radius source with absolute magnitude $M_{\rm abs}=0$. Its apparent magnitude is $m_{\rm app}=M_{\rm abs}-2.5\log_{10}[(10\,{\rm pc}/D_{\rm OS})^2\,\mu]$, where μ is the lensing magnification. Imposing a detection limit $m_{\rm app}=30$ requires $(10\,{\rm Mpc}/D_{\rm OS})^2\,\mu>1$. Including this criterion produces the reduced event number shown in FIG. 6.

As a concrete illustration, take fuzzy dark matter to be the real scalar field analyzed above [14]. If a fraction $f_{\rm BS}$ of dark matter resides in boson stars of mass M, the number density of boson star is $n_a = f_{\rm BS} \rho_{\rm DM}/M$, where $\rho_{\rm DM}$ is the density of dark matter appropriate to the survey volume. Adopting a representative mean stellar number density $n_b \sim 1\,{\rm kpc}^{-3}$ [15], and taking $m=10^{-18}\,{\rm eV}$, $M=10^4\,M_\odot$, and $f_{\rm BS}=10^{-3}$, the expected number of detectable periodic caustic-crossing events in a survey extending to $Z=1\,{\rm Gpc}$ is $N_{\rm evt}\sim \mathcal{O}(10^3)$.

All of the foregoing analysis extends straightforwardly

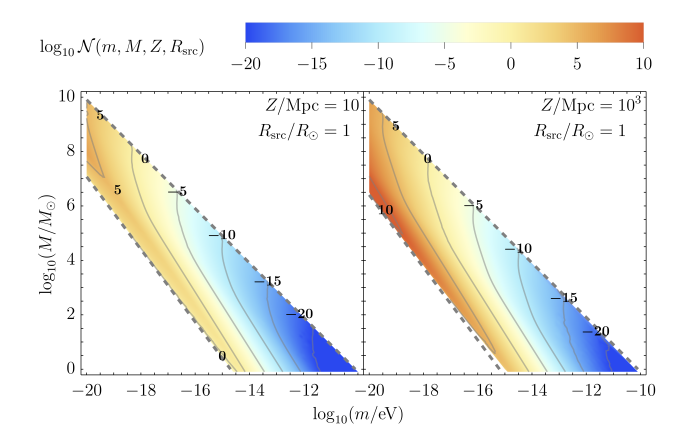


FIG. 6. Reduced event number \mathcal{N} after applying a fiducial detection threshold (see text).

to a massive real scalar with self-interactions [16]. In that setting, axion-like particles provide an especially well-motivated example [17, 18]. Axion stars composed of such particles produce analogous periodic lensing signatures. For a dilute axion star, one finds that $m=10^{-18}\,\mathrm{eV}$ can yield $M=10^4\,M_\odot$ with a boson-star fraction $f_\mathrm{BS}\simeq 0.4$ [19, 20], which in turn implies an expected number of detectable periodic caustic-crossing events of order $N_\mathrm{evt}\sim\mathcal{O}(10^6)$ for a survey depth of $Z=1\,\mathrm{Gpc}$.

Discussions. We have shown that oscillating (realscalar) boson stars can act as strictly periodic gravitational lenses, driving phase-locked photometric and astrometric variability in lensed sources. Their extended nonsingular profiles generate a radial caustic whose size pulsates with the stellar oscillation; a source placed near this caustic undergoes crossings every half period, producing large achromatic magnification spikes and the creation/annihilation of a close pair of bright images. We also derived an event-number estimate and, after imposing a fiducial magnitude cut, found that a measurable subset of such events should be detectable with current facilities. A null search already constrains the abundance of these objects across wide mass ranges. These predictions depend only on the dynamics of long-lived real-scalar condensates and thus provide a clean test of self-gravitating quantum fields in curved spacetime. The framework naturally extends to self-interacting real scalars (e.g., axion-like particles) and ultralight vector bosons [21, 22], for which the core predictions (an oscillating caustic and periodic observables) remain intact.

The periodic caustic-crossing lensing uncovered here constitutes a distinctive target for time-domain astronomy. In the near term, joint analyses that combine Gaiagrade astrometry with high-cadence photometric surveys can already probe periods in the $T\sim 10^2-10^5\,\mathrm{s}$ window and place meaningful null constraints on the number density of oscillating boson stars. Looking ahead, improved microarcsecond astrometry and deeper, faster

time-domain coverage will expand the sensitivity toward lower masses and shorter periods. While we focus on optical gravitational lensing in this work, gravitational waves can also be lensed by oscillating boson stars. As non-static lenses with caustics, they can imprint distinctive signatures on gravitational-wave signals [23, 24], which we leave for future work.

Acknowledgments. X.-Y. Y. is supported in part by the KIAS Individual Grant No. QP090702. R.-G. C. is supported in part by the National Natural Science Foundation of China Grant No. 12588101.

- D. J. Kaup, Klein-Gordon Geon, Phys. Rev. 172, 1331 (1968).
- [2] P. Jetzer, Boson stars, Phys. Rept. 220, 163 (1992).
- [3] F. E. Schunck and E. W. Mielke, General relativistic boson stars, Class. Quant. Grav. 20, R301 (2003), arXiv:0801.0307 [astro-ph].
- [4] S. L. Liebling and C. Palenzuela, Dynamical boson stars, Living Rev. Rel. **26**, 1 (2023), arXiv:1202.5809 [gr-qc].
- [5] L. Visinelli, Boson stars and oscillatons: A review, Int. J. Mod. Phys. D 30, 2130006 (2021), arXiv:2109.05481
 [gr-qc].
- [6] E. Seidel and W. M. Suen, Oscillating soliton stars, Phys. Rev. Lett. 66, 1659 (1991).
- [7] L. A. Urena-Lopez, Oscillatons revisited, Class. Quant. Grav. 19, 2617 (2002), arXiv:gr-qc/0104093.
- [8] L. A. Urena-Lopez, T. Matos, and R. Becerril, Inside oscillatons, Class. Quant. Grav. 19, 6259 (2002).
- M. Alcubierre, R. Becerril, S. F. Guzman, T. Matos,
 D. Nunez, and L. A. Urena-Lopez, Numerical studies of Phi**2 oscillatons, Class. Quant. Grav. 20, 2883 (2003), arXiv:gr-qc/0301105.
- [10] P. Schneider, J. Ehlers, and E. E. Falco, *Gravitational Lenses* (1992).
- [11] M. P. Dabrowski and F. E. Schunck, Boson stars as gravitational lenses, Astrophys. J. 535, 316 (2000), arXiv:astro-ph/9807039.
- [12] S. Mollerach and E. Roulet, Gravitational Lensing and Microlensing (2002).
- [13] P. L. Kelly et al., Extreme magnification of an individual star at redshift 1.5 by a galaxy-cluster lens, Nature Astron. 2, 334 (2018), arXiv:1706.10279 [astro-ph.GA].
- [14] E. G. M. Ferreira, Ultra-light dark matter, Astron. Astrophys. Rev. 29, 7 (2021), arXiv:2005.03254 [astro-ph.CO].
- [15] P. Madau and M. Dickinson, Cosmic Star Formation History, Ann. Rev. Astron. Astrophys. 52, 415 (2014), arXiv:1403.0007 [astro-ph.CO].
- [16] L. A. Urena-Lopez, S. Valdez-Alvarado, and R. Becerril, Evolution and stability phi**4 oscillatons, Class. Quant. Grav. 29, 065021 (2012).
- [17] P. Svrcek and E. Witten, Axions In String Theory, JHEP 06, 051, arXiv:hep-th/0605206.
- [18] A. Arvanitaki, S. Dimopoulos, S. Dubovsky, N. Kaloper, and J. March-Russell, String Axiverse, Phys. Rev. D 81, 123530 (2010), arXiv:0905.4720 [hep-th].
- [19] J. H. Chang, P. J. Fox, and H. Xiao, Axion stars: mass functions and constraints, JCAP 08, 023, arXiv:2406.09499 [hep-ph].

- [20] E. Braaten and H. Zhang, Colloquium: The physics of axion stars, Rev. Mod. Phys. 91, 041002 (2019).
- [21] M. Jain and M. A. Amin, Polarized solitons in higherspin wave dark matter, Phys. Rev. D 105, 056019 (2022), arXiv:2109.04892 [hep-th].
- [22] H.-Y. Zhang, M. Jain, and M. A. Amin, Polarized vector oscillons, Phys. Rev. D 105, 096037 (2022), arXiv:2111.08700 [astro-ph.CO].
- [23] X.-Y. Yang, T. Chen, and R.-G. Cai, Modulations of gravitational waves due to non-static gravitational lenses, JCAP 04, 069, arXiv:2410.16378 [astro-ph.CO].
- [24] J. M. Ezquiaga, R. K. L. Lo, and L. Vujeva, Diffraction around caustics in gravitational wave lensing, Phys. Rev. D 112, 043544 (2025), arXiv:2503.22648 [gr-qc].

End Matter

Oscillating boson-star solution. A minimally coupled massive real scalar field ϕ evolving in a curved background is governed by the Einstein-Klein-Gordon (EKG) equations $G_{ab} = \kappa T_{ab}$ and $\nabla^a \nabla_a \phi = m^2 \phi$. For spherical symmetry, it is convenient to introduce the dimensionless variables $\tilde{t} \equiv mt$, $\tilde{r} \equiv mr$, and $\tilde{\phi} \equiv \sqrt{\kappa} \phi$, in terms of which the EKG equations read

$$\frac{A'}{A} = \frac{1-A}{\tilde{r}} + \frac{\tilde{r}}{2} \left(\frac{A}{B}\dot{\tilde{\phi}}^2 + \tilde{\phi}'^2 + A\tilde{\phi}^2\right),\tag{9a}$$

$$\frac{B'}{B} = \frac{A-1}{\tilde{r}} + \frac{\tilde{r}}{2} \left(\frac{A}{B}\dot{\tilde{\phi}}^2 + \tilde{\phi}'^2 - A\tilde{\phi}^2\right),\tag{9b}$$

$$\ddot{\tilde{\phi}} = (\frac{\dot{B}}{2B} - \frac{\dot{A}}{2A})\dot{\tilde{\phi}} + \frac{B}{A}\tilde{\phi}'' + (\frac{B'}{2B} - \frac{A'}{2A} + \frac{2}{\tilde{r}})\frac{B}{A}\tilde{\phi}' - B\tilde{\phi},$$
(9c)

where overdots and primes denote derivatives with respect to \tilde{t} and \tilde{r} , respectively. Substituting the solutions of form (10) into the EKG equations (9),

$$A(\tilde{t}, \tilde{r}) = 1 + \sum_{j=0}^{j_{\text{max}}} A_{2j}(\tilde{r}) \cos(2j\tilde{\omega}\tilde{t}), \tag{10a}$$

$$B(\tilde{t}, \tilde{r}) = 1 + \sum_{j=0}^{j_{\text{max}}} B_{2j}(\tilde{r}) \cos(2j\tilde{\omega}\tilde{t}), \tag{10b}$$

$$\tilde{\phi}(\tilde{t}, \tilde{r}) = \sum_{j=1}^{j_{\text{max}}} \tilde{\phi}_{2j-1}(\tilde{r}) \cos([2j-1]\tilde{\omega}\tilde{t}), \tag{10c}$$

with $\tilde{\omega} \equiv \omega/m$. Matching terms of the same frequency yields a set of coupled ordinary differential equations for the radial coefficients $A_{2j}(\tilde{r})$, $B_{2j}(\tilde{r})$, and $\tilde{\phi}_{2j-1}(\tilde{r})$. We retain only the leading oscillatory terms and set $j_{\max} = 1$, because the Fourier expansion converges rapidly. The boundary conditions are: (i) asymptotic flatness requires $\tilde{\phi}|_{\tilde{r}\to\infty}\to 0$ and $\{A,B\}|_{\tilde{r}\to\infty}\to 1$; (ii) central regularity implies $\partial_{\tilde{r}}\tilde{\phi}|_{\tilde{r}=0}=0$ and $A|_{\tilde{r}=0}=1$. A representative solution with central amplitude $\tilde{\phi}_1(0)=0.13$ is shown in FIG. 7; it has dimensionless mass $\tilde{M}\approx 0.5$ and frequency $\tilde{\omega}\approx 0.95$.

In the small-amplitude regime $\phi_1(0) \ll 1$, the equations exhibit an approximate scale invariance. Specifically, for any $\ell > 0$,

$$\{ \tilde{r}, \tilde{\phi}_1, B_0, B_2, A_0, A_2 \}
\to \{ \ell^{-1} \tilde{r}, \ell^2 \tilde{\phi}_1, \ell^2 B_0, \ell^2 B_2, \ell^2 A_0, \ell^4 A_2 \}, \tag{11}$$

which underlies the familiar mass-radius scaling of oscillating boson-star solutions.

Deflection angle. Photon trajectories follow null geodesics. Restricting to the equatorial plane $(\vartheta = \pi/2)$,

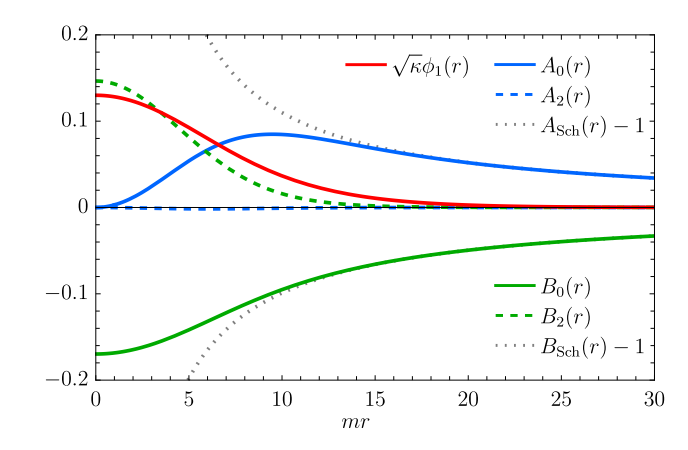


FIG. 7. Representative oscillating boson-star solution with $\tilde{\phi}_1(0)=0.13$, giving $\tilde{M}\approx 0.5$ and $\tilde{\omega}\approx 0.95$. Here $A_{\rm Sch}$ and $B_{\rm Sch}$ denote the metric functions of the Schwarzschild metric.

the geodesic equations read

$$0 = t'' + \frac{\partial_r B}{B} t' r' + \frac{\partial_t A}{2B} r'^2 + \frac{\partial_t B}{2B} t'^2, \tag{12a}$$

$$0 = r'' + \frac{\partial_t A}{A} t' r' + \frac{\partial_r B}{2A} t'^2 + \frac{\partial_r A}{2A} r'^2 - \frac{r}{A} \varphi'^2, \quad (12b)$$

$$0 = \varphi'' + \frac{2}{r}r'\varphi',\tag{12c}$$

where primes denote derivatives with respect to an affine parameter ς along the geodesic. A given null geodesic can be specified by the time \hat{t} and radius \hat{r} of closest approach. We integrate the geodesic equations with initial data

$$\{t(\varsigma), r(\varsigma), \vartheta(\varsigma), \varphi(\varsigma)\}\Big|_{\varsigma=0} = \{\hat{t}, \hat{r}, \pi/2, 0\},$$
 (13a)

$$\left\{ \frac{\mathrm{d}t}{\mathrm{d}\varsigma}, \frac{\mathrm{d}r}{\mathrm{d}\varsigma}, \frac{\mathrm{d}\vartheta}{\mathrm{d}\varsigma}, \frac{\mathrm{d}\varphi}{\mathrm{d}\varsigma} \right\} \bigg|_{\varsigma=0} = \{1, 0, 0, \frac{\sqrt{B(\hat{t}, \hat{r})}}{\hat{r}}\}, \quad (13b)$$

which fix the trajectory and its impact parameter. The deflection angle is then

$$\hat{\alpha}(\hat{t}, \hat{r}) \equiv \varphi(+\infty) - \varphi(-\infty) - \pi. \tag{14}$$

In FIG. 8, we show the numerical results of the deflection angle for a representative oscillating boson star with $\tilde{M}=0.5$, together with the broken power-law parametrization in Eq. (3). The parametrization reproduces the numerical results to high accuracy.

Caustic and critical curve. Caustics and critical curves are conveniently characterized by the image magnification,

$$\mu = \left(\frac{\sin \beta}{\sin \theta} \frac{\mathrm{d}\beta}{\mathrm{d}\theta}\right)^{-1},\tag{15}$$

which factorizes into a tangential and a radial piece,

$$\mu_{\rm t} = \left(\frac{\sin \beta}{\sin \theta}\right)^{-1},\tag{16a}$$

$$\mu_{\rm r} = \left(\frac{\mathrm{d}\beta}{\mathrm{d}\theta}\right)^{-1}.\tag{16b}$$

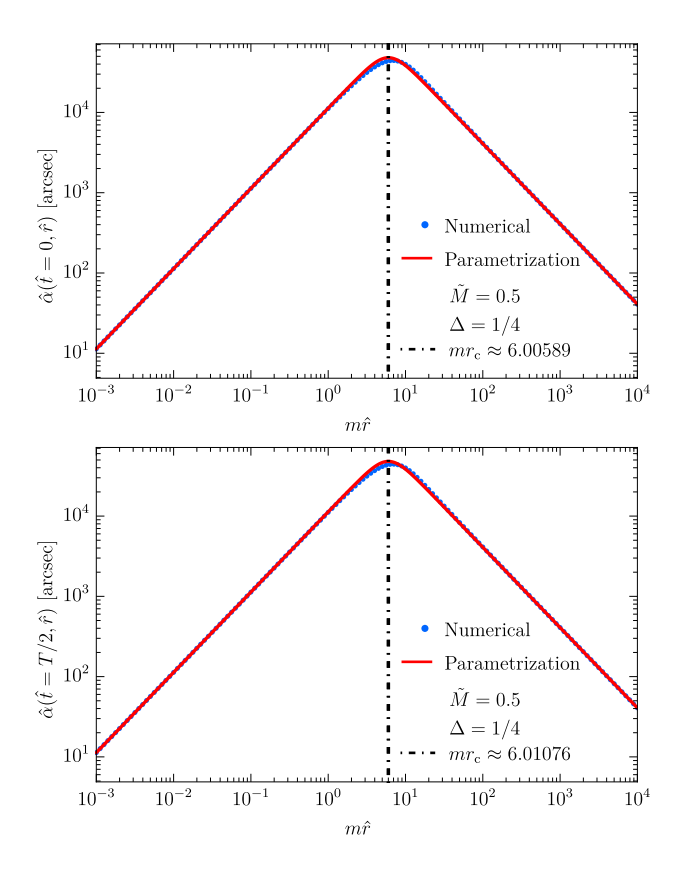


FIG. 8. Numerical results and broken power-law parametrization of the deflection angle for the oscillating boson star with $\tilde{M}=0.5.$

Singularities of $\mu_{\rm t}$ and $\mu_{\rm r}$ define the tangential and radial critical curves in the image plane, respectively. Their mappings into the source plane are the corresponding caustics. In particular, the tangential critical curve (the Einstein ring) is located at $x_{\rm Ein}$, while the radial critical curve lies at $x_{\rm cri}$ with an associated source-plane radial caustic at $y_{\rm cau}$. Using the dimensionless lens equation, one obtains $y_{\rm cau}(\nu)$ together with $x_{\rm cri}(\nu)$ and $x_{\rm Ein}(\nu)$ as functions of the parameter ν . These relations are shown in FIG. 9. As evident in the figure, the radial caustic size $y_{\rm cau}$ decreases monotonically with increasing ν . Since $\nu(t)$ is periodic, the radial caustic therefore pulsates in and out with the same period, a key driver of the periodic caustic-crossing lensing phenomenology.

Event number. Assuming the survey volume extends out to a distance Z, and denoting by n_a and n_b the number densities of oscillating boson stars and sources, respectively. The number of lenses in a spherical shell of radius $D_{\rm OL}$ and thickness ${\rm d}D_{\rm OL}$ is $n_a \, 4\pi D_{\rm OL}^2 {\rm d}D_{\rm OL}$. For a given $D_{\rm OL}$, the number of sources that both satisfy $D_{\rm OS} > D_{\rm OL}^2/(D_{\rm OL} - r_{\rm cS})$ and fall within the angular

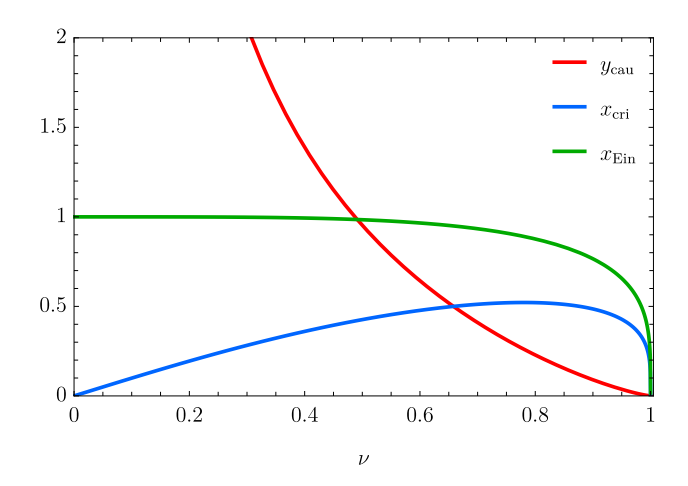


FIG. 9. Radial caustic $y_{\rm cau}$ (source plane), radial and tangential critical curves $x_{\rm cri}$ and $x_{\rm Ein}$ (image plane) as functions of ν .

window $\beta_{\min} < \beta_{\rm src} < \beta_{\max}$ is

$$\int_{D_{\rm OL}}^{Z} dD_{\rm OS} \left\{ n_b \Theta (D_{\rm OS} - \frac{D_{\rm OL}^2}{D_{\rm OL} - r_{\rm cS}}) \times 2\pi D_{\rm OS}^2 \, \max \left[0, \, \cos \beta_{\rm min} - \cos \beta_{\rm max} \right] \right\}, \tag{17}$$

where $\Theta(x)$ is the Heaviside step function. Imposing the remaining condition $D_{\rm OL} > r_{\rm cS}$, the expected number of periodic caustic-crossing lensing events is

$$N_{\text{evt}} = \int_{0}^{Z} dD_{\text{OL}} \left\{ n_a \Theta(D_{\text{OL}} - r_{\text{cS}}) 4\pi D_{\text{OL}}^2 \right.$$

$$\times \int_{D_{\text{OL}}}^{Z} dD_{\text{OS}} \left\{ n_b \Theta(D_{\text{OS}} - \frac{D_{\text{OL}}^2}{D_{\text{OL}} - r_{\text{cS}}}) \right.$$

$$\times 2\pi D_{\text{OS}}^2 \max \left[0, \cos \beta_{\min} - \cos \beta_{\max} \right] \right\}.$$
(18)

Requiring the presence of a radial caustic ($\nu < 1$) sets a lower bound on the mass of an oscillating boson star, $M > r_{\rm c}^2/(4D)$, where $D \equiv D_{\rm OL}(D_{\rm OS}-D_{\rm OL})/D_{\rm OS}$. Invoking the scale invariance of EKG equations in the small-amplitude regime, one finds $\tilde{r}_{\rm c} \propto M^{-1}$, which implies $r_{\rm c} \propto M^{-1}m^{-2}$. Consequently, the minimum mass capable of producing an oscillating caustic is

$$M_{\rm min} \approx 1.6 \times 10^7 \, M_{\odot} \left(\frac{1 \,\mathrm{Mpc}}{D}\right)^{1/3} \left(\frac{10^{-20} \,\mathrm{eV}}{m}\right)^{4/3},$$
(19)

For the representative geometry $Z=D_{\rm OS}=2D_{\rm OL}$ (so that D=Z/4), this becomes

$$M_{\rm min} \approx 1.6 \times 10^7 \, M_{\odot} \left(\frac{Z/4}{1 \,\rm Mpc}\right)^{-1/3} \left(\frac{m}{10^{-20} \,\rm eV}\right)^{-4/3}.$$
 (20)